VLBA ACQUISITION MEMO 390

MASSACHUSETTS INSTITUTE OF TECHNOLOGY
HAYSTACK OBSERVATORY
WESTFORD, MASSACHUSETTS 01886

May 10, 1995

Telephone: *508-692-4764*
Fax: *617-981-0590*

To: VLBA Data Acquisition Group
From: Sinan Müftü
Subject: Modelling and Evaluation of the Current Head-Stack

1 Introduction

The purpose of this memorendum is to present a mathematical model for evaluating the head-tape interface of the VLBA recorders. Theoretical studies by Rogers have included many of the effects that this model has [6]. Determination of an "equilibrium radius" in that and similar studies outlined in the VLBA Acquistion Memo Series is a capability not included in this model. Instead this model assumes that the equilibrium radius is known apriori. The slip flow effect in the Reynolds equation for air lubrication in submicron head-tape gaps, and asperity compliance for full tape-head contact are included in this study.

After briefly introducing the governing equations of the model, we evaluate the current head geometry with and without the wedges that exist on the head-stack.

2 Governing Equations of the Model

The geometry of magnetic recording head that is modeled is shown in Figure 1 and specified by [1]. We are assume that the tape is wrapped around a head that has a radius, R. We are approximate the worn parts of the head at the edges by assuming that the tape is tangent to the head at the location $\theta = (\theta_{L,R} - \theta_w)$.

In the model the tape is modeled as a cylindrical segmented shell,

$$D\frac{d^4w}{dx^4} + kw + (\rho_a V_x^2 - T_x)\frac{d^2w}{dx^2} = p(h) - P_a + P_c(h) - P_{bw} \tag{1}$$

The parameters appearing in this equation are explained in Table 1, except for the following,

$D = \frac{Ec^3}{12(1-\nu^2)}$, bending rigidity of the tape,

w tape displacement in the normal direction,

h head-tape spacing,

p air pressure,

P_c contact pressure,

The shell stiffness, $k(= \frac{Ec}{R^2(1-\nu^2)})$, and the belt-wrap pressure, $P_{bw} = (\frac{T_x}{R})$, are non-zero only in the wrap zone, $-(\theta_L - \theta_w) \leq \theta \leq (\theta_R - \theta_w)$.

The effect of air in the head-tape interface is modeled by the Reynolds equation with first order slip flow correction,

$$\frac{\partial}{\partial x}(ph^3\frac{\partial p}{\partial x}) + 6\lambda P_a\frac{\partial}{\partial x}(h^2\frac{\partial p}{\partial x}) = 6\mu(V_x\frac{\partial ph}{\partial x}) \tag{2}$$

The slip flow assumption is valid for the Knudsen number ($Kn = \frac{h}{\lambda}$) of 1/15 [2].

The contact pressure between the tape and the head is modeled by the following asperity compliance function,

$$P_c = f(h)H(-(h-\sigma_t)) \tag{3}$$

where, $H(-(h-\sigma_t)$ is the Heaviside step function which insures that the function $f(h)$ is applied only if the head tape spacing falls below the asperity engaging height, σ_t. A variety of functions can be used for $f(h)$ including the theoretically derived Greenwood and Williamson [3] model or the empirically derived, parabolic, asperity compliance function [4]. In this memo we use the latter approach with $f(h) = P_o(1-\frac{h}{\sigma_t})^2$.

These three equations form a system of non-linear equations. They are solved using a modified Newton-Raphson algorithm as described in [5].

3 Results

We analyze the head-stack in two different parts. In the first part we look at the effect of the head step, only. In the second part we include into our analysis the wedges on the leading and trailing edges of the head-step. These are presented in the next two subsections.

3.1 The Effect of the Head Step

In this part we focus only on the effect of the head-step. Therefore, the parameters S_w, S_L are set to zero and θ_h is set to 90^o. Other parameters describing the problem are given in Table 1. This case is similar to a situation where the wedge is does not exist.

For a fixed head geometry the head-tape spacing is a strong function of the tape speed, V_x, and the tape tension, T_x. We study the effect of these two parameters on the head tape spacing for a combination of $V_x = 2, 4, 6, 8, 10m/s$ and $T_x = 4, 8, 12, 16" H_2O$.

Head Without Any Wear

Our simulations showed that when the wear angle, θ_w is zero the head and the tape do not become separated for upto a tape speed of $20m/s$, and contact is maintained. However, it would be unrealistic to expect that this situation would be valid throughout the life of the head. This is due to the fact that the edges of the head are more suspect to wear due to high localized contact pressures.

The Effect of Edge Wear on Performance

We assume that initially the edges of the head are worn out faster than the rest of the head. As a first approximation this rounding is modeled by recessing the tangency points toward the inside of the tape by the *wear angle*, θ_w[1]. Our simulations showed that flying

[1]The wear would also, change the radius of the head at these locations, but we did not include that effect. A more complete wear model is required to find the worn shape.

does not occur when $\theta_w < 0.1^o$ for this geometry. However for higher wear angles simulations predicted flying for high velocities and low tensions.

Figures 2 and 3 show the head tape spacing at the recording gap, $\theta = 0$, as a function of the ratio V_x/T_x. In Figure 2 the wear angle is 0.2^o and in Figure 3 it is 0.15^o. These two figures show that for the lower amount of wear the flying occurs at tape speeds 8 and 10 m/s, whereas for the higher amount of wear flying occurs even at 4 m/s.

The model can also predict the head tape spacing when the tape is in contact with the head. In this region the tape is supported by the compliance of the asperities on its back side. As the *wrap pressure* is increased by increasing the tension we see that the head tape gap decreases slightly. (See Figures 2 and 3.) However, since the asperities are quite stiff this reduction is very modest.

The Interface Conditions for Mixed and Full Lubrication Cases

In Figure 4 we show the interface conditions for $V_x = 6m/s$ and wear angle of 0.15^o. Flying does not occur for these parameters as evidenced by the fact that the head tape spacing, h, and the tape displacement, w, are below the asperity contact level σ_t. The tape is supported by a combination of the contact and air pressures. This lubrication regime is called the *mixed lubrication* regime. This figure shows that as the tension is increased the air pressure in the interface hardly changes, but the contact pressure increases considerably[2].

In Figure 5 the interface conditions for the same head at 8 m/s tape speed are shown. Here we see that at the lowest tension (4 in H20) the tape clears the asperity peaks and flying occurs. We call this regime the *full lubrication* regime. The air pressure profiles are nearly the same as before, but in the case where flying occurs the pressure is lower on the entry side than that of the middle region of the tape. Also note in these figures that the length of the constant gap part of the tape displacement decreases as the tape starts to fly.

3.2 The Combined Effect of the Head Step and the Wedges

The term wedge is used to describe the flat parts of the head stack before and after the head-step. In this case the head looks exactly like the case given in Figure 1, with parameters as given in Table 1.

Our analysis of this type of head showed that for the given geometry the effect of the leading and trailing side wedges is quite strong in initiating tape flying except when $\theta_w = 0$. In this case, where the edges are not rounded, the tape does not fly. Figure 6 shows the conditions at the interface for $10m/s$ tape speed, and 4" H_2O vacuum pressure. We see in this figure that even at a very fast tape speed the amount of air that enters the head-tape interface is insignificant.

However, this situation changes dramatically when we introduce a very small amount of wear by rounding the edges of the head-step. A wear angle of $\theta_w = 0.05^o$ is sufficient to initiate flying at a tape speed of $8m/s$. For higher wear angles, the model predicted flying even at $2m/s$ tape speed. Figure 7 shows the interface conditions for 0.05^o wear angle. For this case, the tape tension was set by 4" H_2O vacuum pressure.

[2]The equilibrium of the tape requires that

$$\int_0^{L_s} (p + P_c)dx = \int_0^{L_s} (F_b + \frac{T_x}{R})dx \tag{4}$$

where, F_b is the internal force supported by the bending and the in-plane resistance of the tape.

We see in the air pressure profiles that on the leading side wedge, the air pressure becomes super-ambient on the entry side of the head-step. This was predicted by Rogers [6]. On the trailing side wedge, the air presure is sub-ambient only for $V = 2/ms$ case, where there is total contact with the head. For higher tape speeds the air pressure on the trailing side wedge is super-ambient. The lack of the exit side "wiggle" on the air pressure profile is a surprising result, compared to the classical foil bearing configurations where the tape is wrapped around a cylindrical head with generous leading and trailing edge angles. See for example Stahl, et al. [6]. We attribute this finding to the shape that the tape deforms into when fully or partially "flying" in this head-stack configuration.

4 Conclusions

This study showed that the wedges on the leading and trailing sides of the head-step contribute to head-tape separation above the asperity heights (flying). Eventhough, more parametric studies are required, our first impression is that in the future head designs elimination of the wedges, or increase of the 15° wedge angle would improve the head-tape contact even for a larger amount of edge wear.

5 References

1. Hinteregger, H. "Headstack Specification for Mk3A/VLBA/Mk4 Compatibility," VLBA Acquisition Memo # 352, MIT, Haystack Observatory, March 1993.
2. Hamrock, B.J. *Fundamentals of Fluid Film Lubrication*, McGraw-Hill, NY, 1994.
3. Bhushan, B. *Tribology and Mechanics of Magnetic Storage Devices*, Springer-Verlag, 1990.
4. Lacey, C. *The Head/Tape Interface*, PhD-thesis, UCSD, La Jolla, CA. 1992.
5. Müftü, S., Benson, R.C., "Modelling the Transport of Paper Webs Including the Paper Permeability Effects," submitted for review for the Proceedings of the ISPS at the ASME, WAM in San Fransisco, CA, November 1995.
6. Rogers, A.E.E. *Theoretical Model for Head Flying*, VLBA Acquisition Memo # 264, MIT, Haystack Observatory, July 1991.
7. Stahl, K.J., White, J.W., Deckert, K.L., "Dynamic response of self-acting foil bearings," *IBM Journal of Research and Development*, pp 513-520, 1974.

Head-Geometry		Head Step Only	With The Wedges
R	Guide Radius	$2.54mm$	$2.54mm$
$\theta_L = \theta_R$	See Fig. 1a	3.4^o	3.4^o
$\theta_w = \theta_w$	Wear Angle	$0^o - 0.15^o$	$0^o - 0.15^o$
S_h	Step-height	1 mm	$137.16\mu m$
S_w	Step-width	0	$231\mu m$
S_L	Side length	0	$500\mu m$
θ_h	Side Angle	90^o	22^o
L_{ss}	See Fig. 1a	$1cm$	$1cm$
Tape			
T_x	Web tension	31.63-126.54 N/m	
		4-16 in. H2O	
V_x	Web speed	variable	
E	Young's Modulus	4 GPa	
μ	Poisson's ratio	0.3	
ρ	Density	1400 kgm^{-3}	
c	Web thickness	15.2 μm	
σ_t	Asp. Cont. Height	50 nm	
P_o	Asp. Compl. Cons.	10 MPa	
Air			
ν	Air viscosity	$1.85 \times 10{-}5Nsm^{-2}$	
λ	Mean free path	$63.5nm$	
P_a	Ambient pressure	$101.3kPa$	

Table 1: Variables used in Figures 1-4.

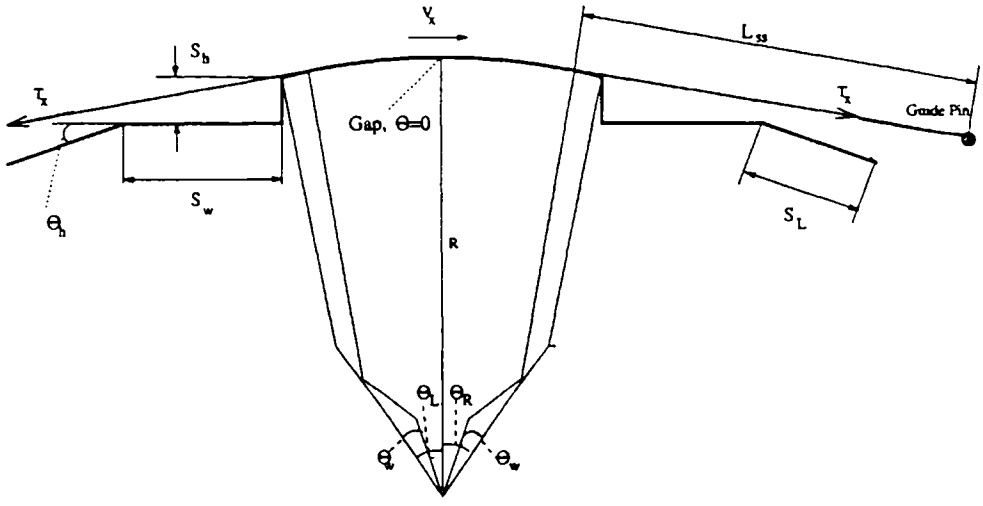

Figure 1: The schematic side view of the head-tape assembly. See Table 1 for the dimensions.

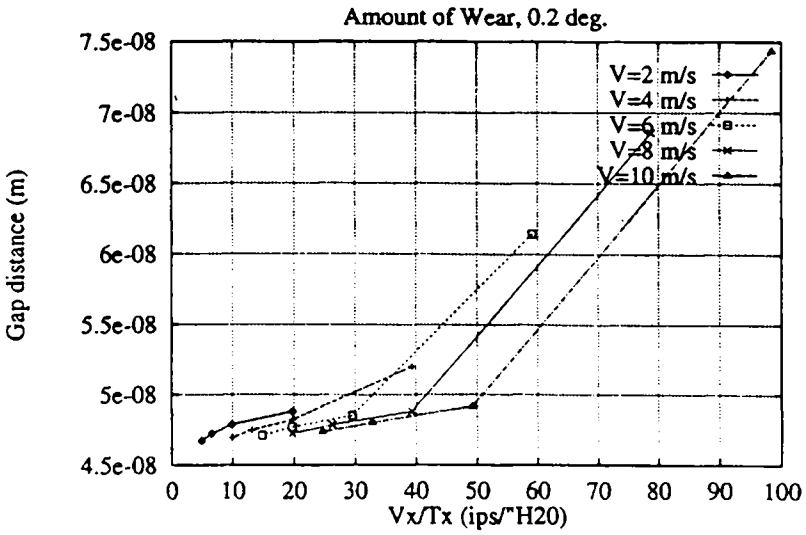

Figure 2: The flying height at the gap as a function of the ratio V_x/T_x. Note that $\theta_{t1} \geq 1.6$ does not show flying.

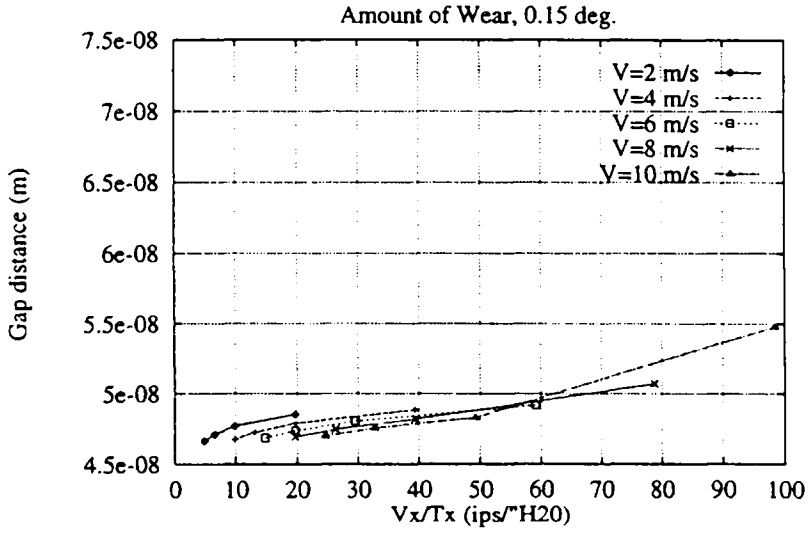

Figure 3: The flying height at the gap as a function of the ratio V_x/T_x. Note that $\theta_{t1} \geq 1.6$ does not show flying.

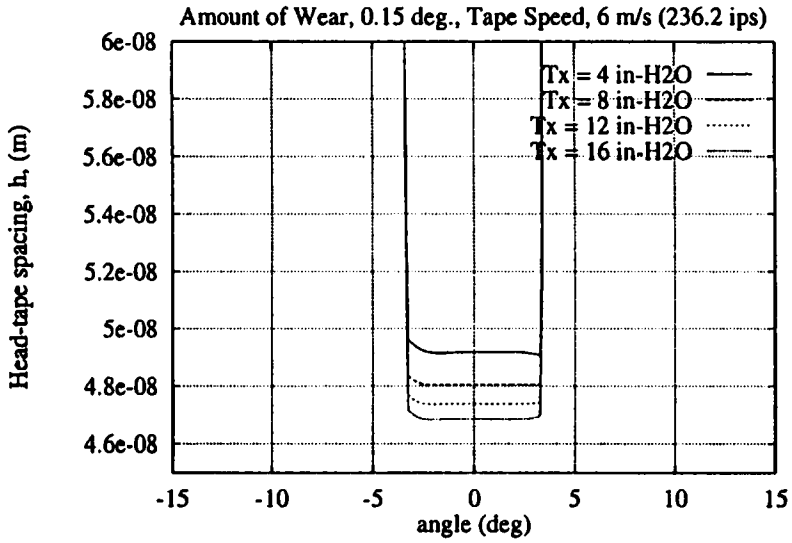
Amount of Wear, 0.15 deg., Tape Speed, 6 m/s (236.2 ips)
Head-tape spacing, h, (m)
6e-08
5.8e-08
5.6e-08
5.4e-08
5.2e-08
5e-08
4.8e-08
4.6e-08
-15
-10
-5
0
5
10
15
angle (deg)
Tx = 4 in-H2O
Tx = 8 in-H2O
Tx = 12 in-H2O
Tx = 16 in-H2O

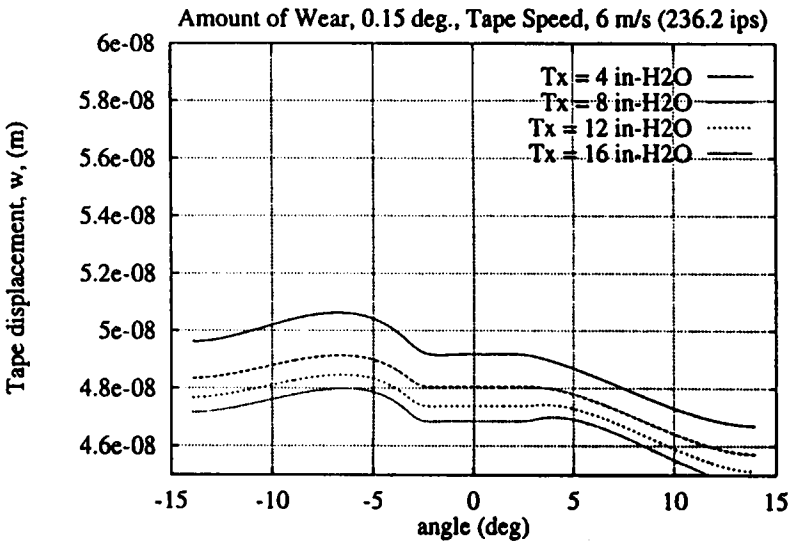
Amount of Wear, 0.15 deg., Tape Speed, 6 m/s (236.2 ips)
Tape displacement, w, (m)
6e-08
5.8e-08
5.6e-08
5.4e-08
5.2e-08
5e-08
4.8e-08
4.6e-08
-15
-10
-5
0
5
10
15
angle (deg)
Tx = 4 in-H2O
Tx = 8 in-H2O
Tx = 12 in-H2O
Tx = 16 in-H2O

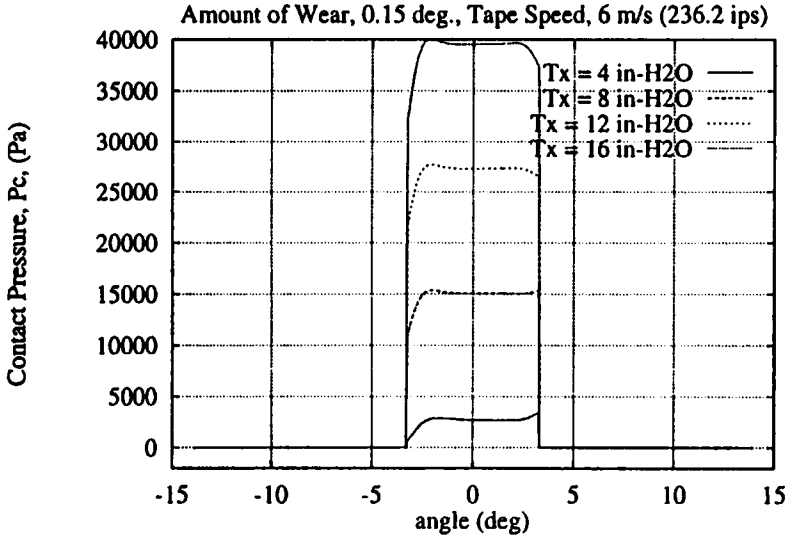
Amount of Wear, 0.15 deg., Tape Speed, 6 m/s (236.2 ips)
Contact Pressure, Pc, (Pa)
40000
35000
30000
25000
20000
15000
10000
5000
0
-15
-10
-5
0
5
10
15
angle (deg)
Tx = 4 in-H2O
Tx = 8 in-H2O
Tx = 12 in-H2O
Tx = 16 in-H2O

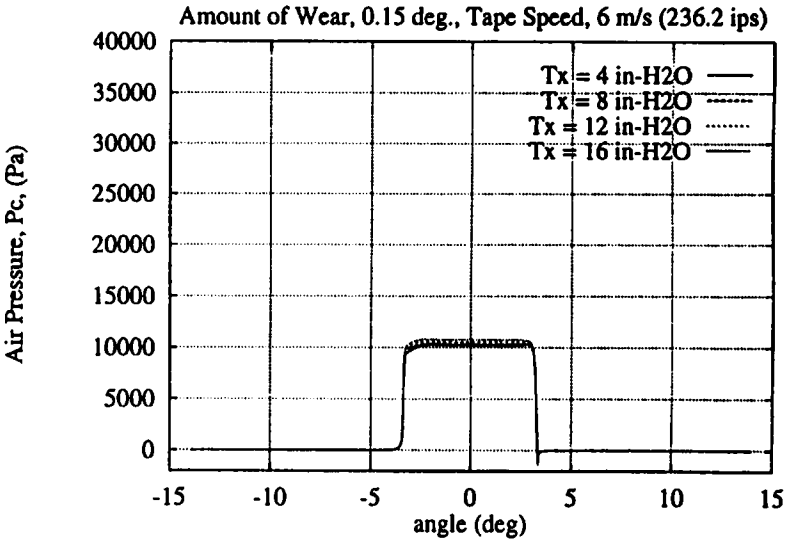
Amount of Wear, 0.15 deg., Tape Speed, 6 m/s (236.2 ips)
Air Pressure, Pc, (Pa)
40000
35000
30000
25000
20000
15000
10000
5000
0
-15
-10
-5
0
5
10
15
angle (deg)
Tx = 4 in-H2O
Tx = 8 in-H2O
Tx = 12 in-H2O
Tx = 16 in-H2O

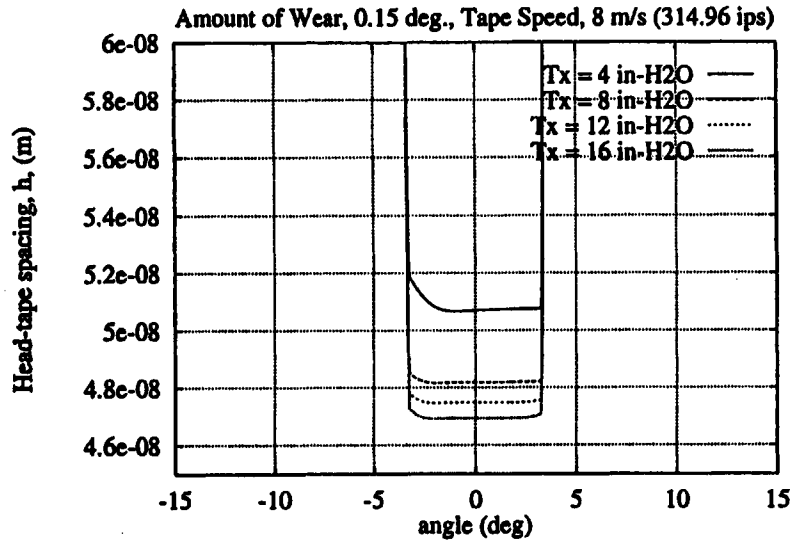
Amount of Wear, 0.15 deg., Tape Speed, 8 m/s (314.96 ips)
Head-tape spacing, h, (m)
6e-08
5.8e-08
5.6e-08
5.4e-08
5.2e-08
5e-08
4.8e-08
4.6e-08
-15
-10
-5
0
5
10
15
angle (deg)
Tx = 4 in-H2O
Tx = 8 in-H2O
Tx = 12 in-H2O
Tx = 16 in-H2O

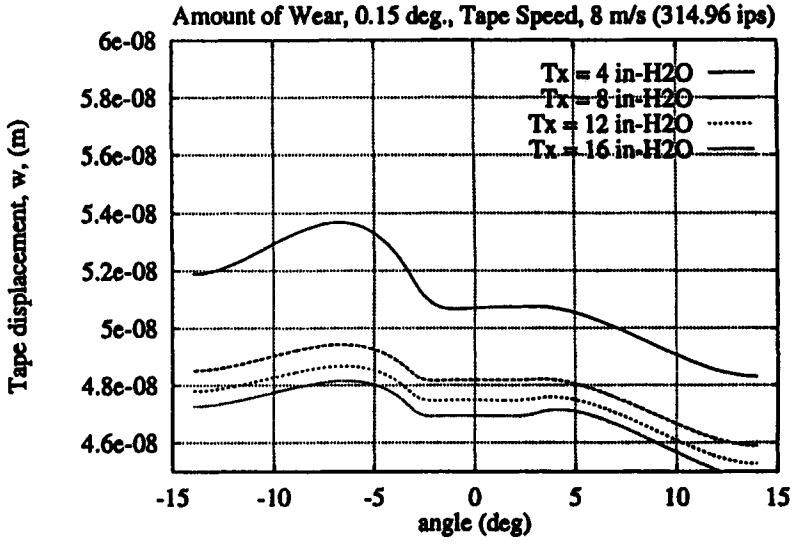
Amount of Wear, 0.15 deg., Tape Speed, 8 m/s (314.96 ips)
Tape displacement, w, (m)
6e-08
5.8e-08
5.6e-08
5.4e-08
5.2e-08
5e-08
4.8e-08
4.6e-08
-15
-10
-5
0
5
10
15
angle (deg)
Tx = 4 in-H2O
Tx = 8 in-H2O
Tx = 12 in-H2O
Tx = 16 in-H2O

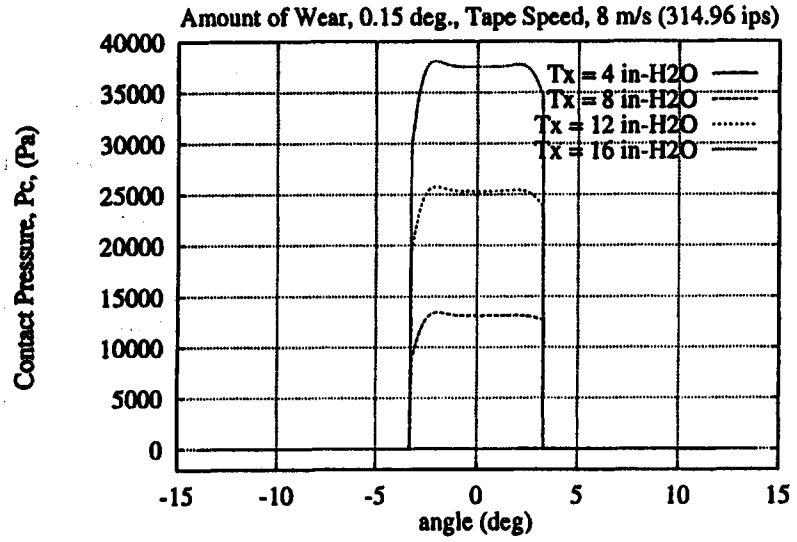
Amount of Wear, 0.15 deg., Tape Speed, 8 m/s (314.96 ips)
Contact Pressure, Pc, (Pa)
40000
35000
30000
25000
20000
15000
10000
5000
0
-15
-10
-5
0
5
10
15
angle (deg)
Tx = 4 in-H2O
Tx = 8 in-H2O
Tx = 12 in-H2O
Tx = 16 in-H2O

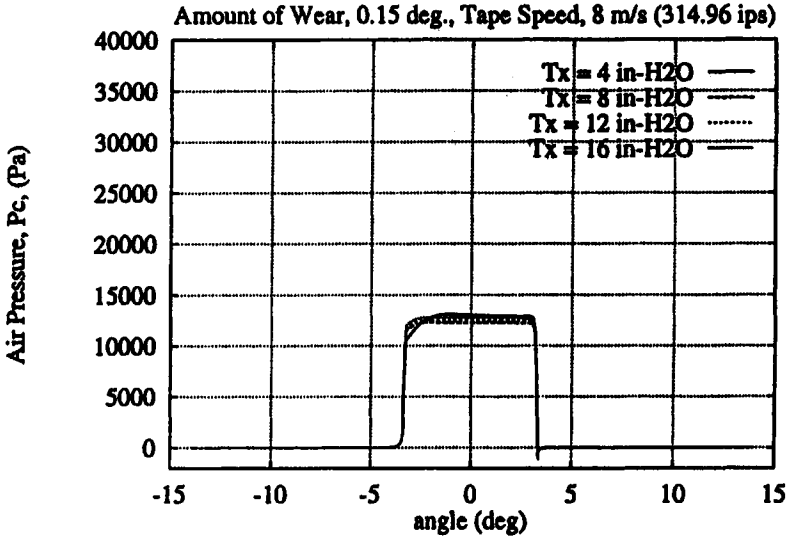
Amount of Wear, 0.15 deg., Tape Speed, 8 m/s (314.96 ips)
Air Pressure, Pc, (Pa)
40000
35000
30000
25000
20000
15000
10000
5000
0
-15
-10
-5
0
5
10
15
angle (deg)
Tx = 4 in-H2O
Tx = 8 in-H2O
Tx = 12 in-H2O
Tx = 16 in-H2O

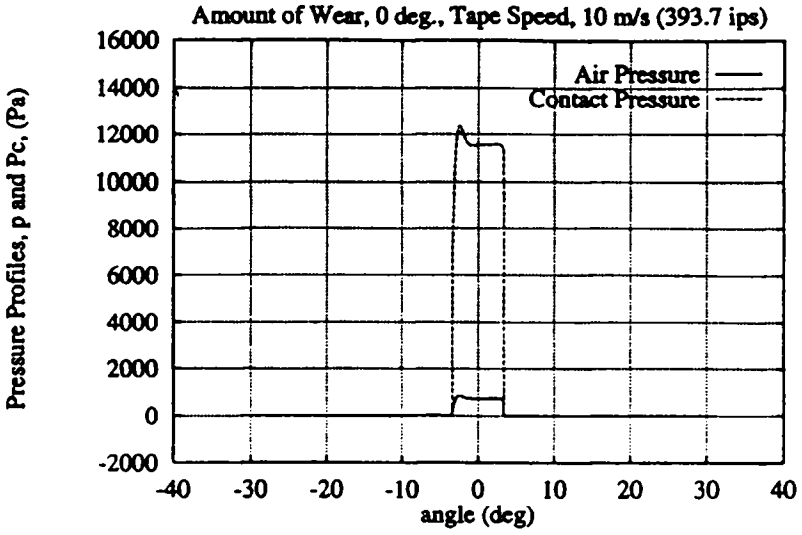
Amount of Wear, 0 deg., Tape Speed, 10 m/s (393.7 ips)
Air Pressure
Contact Pressure
Pressure Profiles, p and Pc, (Pa)
16000
14000
12000
10000
8000
6000
4000
2000
0
-2000
-40
-30
-20
-10
0
10
20
30
40
angle (deg)

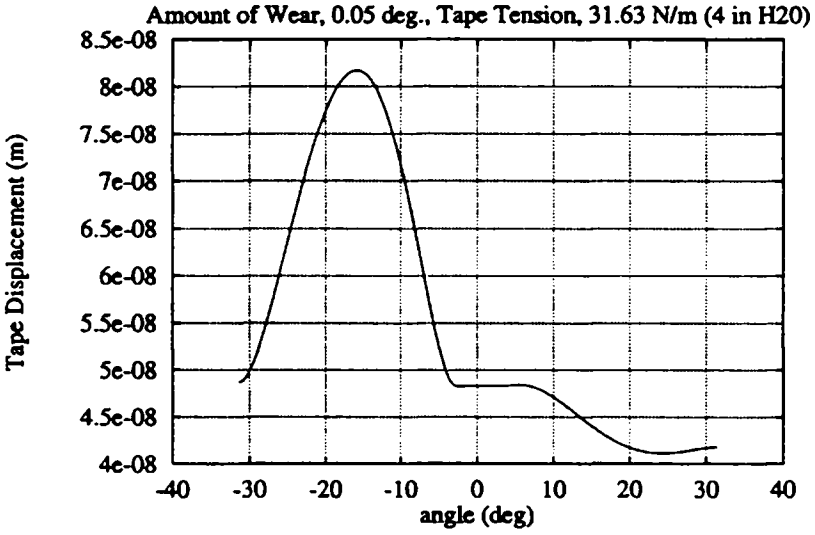
Amount of Wear, 0.05 deg., Tape Tension, 31.63 N/m (4 in H20)
Tape Displacement (m)
8.5e-08
8e-08
7.5e-08
7e-08
6.5e-08
6e-08
5.5e-08
5e-08
4.5e-08
4e-08
-40
-30
-20
-10
0
10
20
30
40
angle (deg)

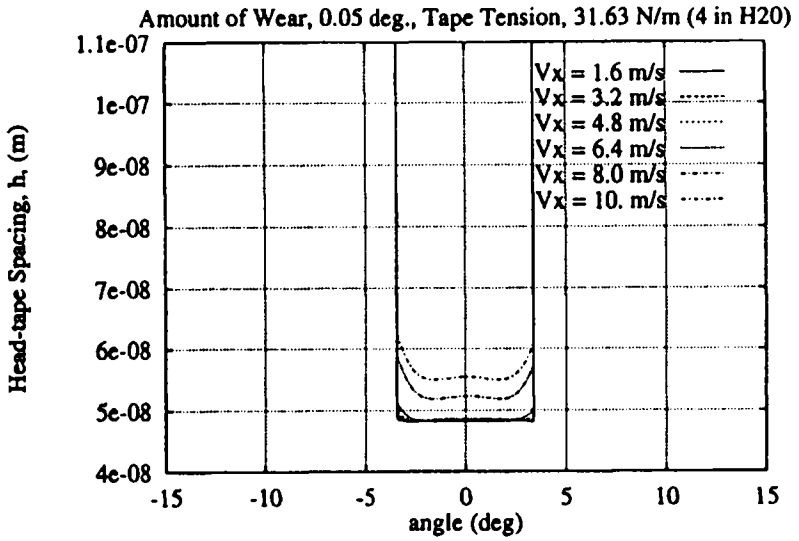
Amount of Wear, 0.05 deg., Tape Tension, 31.63 N/m (4 in H20)
Head-tape Spacing, h, (m)
1.1e-07
1e-07
9e-08
8e-08
7e-08
6e-08
5e-08
4e-08
-15
-10
-5
0
5
10
15
angle (deg)
Vx = 1.6 m/s
Vx = 3.2 m/s
Vx = 4.8 m/s
Vx = 6.4 m/s
Vx = 8.0 m/s
Vx = 10. m/s

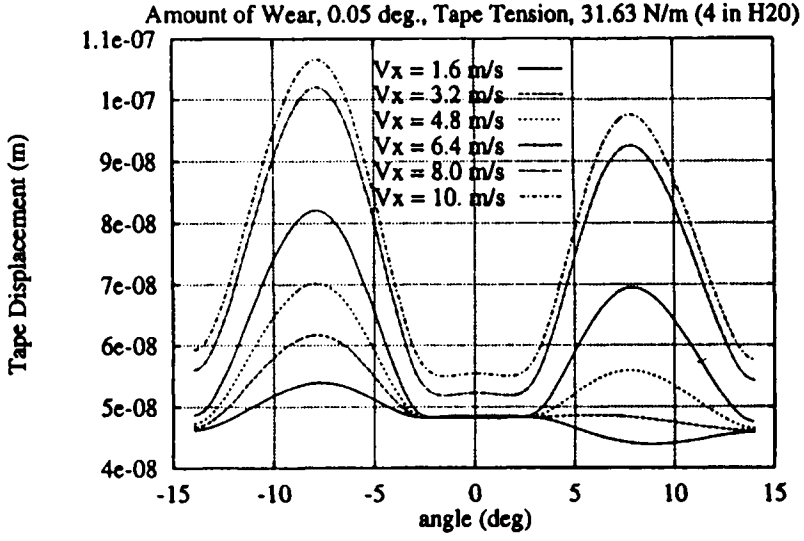
Amount of Wear, 0.05 deg., Tape Tension, 31.63 N/m (4 in H20)
Tape Displacement (m)
1.1e-07
1e-07
9e-08
8e-08
7e-08
6e-08
5e-08
4e-08
-15
-10
-5
0
5
10
15
angle (deg)
Vx = 1.6 m/s
Vx = 3.2 m/s
Vx = 4.8 m/s
Vx = 6.4 m/s
Vx = 8.0 m/s
Vx = 10. m/s

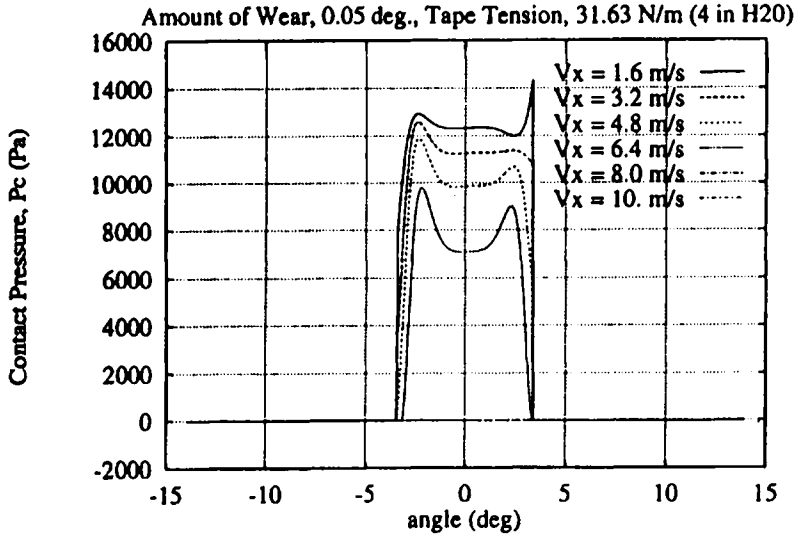
Amount of Wear, 0.05 deg., Tape Tension, 31.63 N/m (4 in H20)
Contact Pressure, Pc (Pa)
16000
14000
12000
10000
8000
6000
4000
2000
0
-2000
-15
-10
-5
0
5
10
15
angle (deg)
Vx = 1.6 m/s
Vx = 3.2 m/s
Vx = 4.8 m/s
Vx = 6.4 m/s
Vx = 8.0 m/s
Vx = 10. m/s

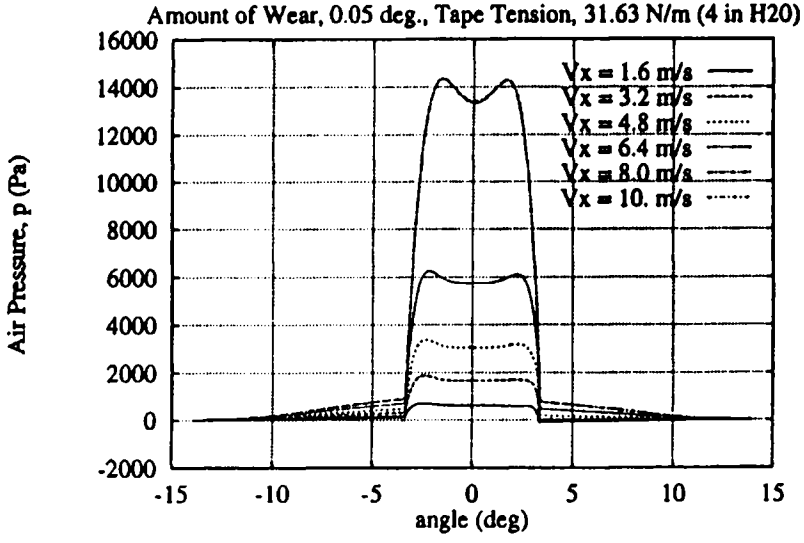
Amount of Wear, 0.05 deg., Tape Tension, 31.63 N/m (4 in H20)
Air Pressure, p (Pa)
16000
14000
12000
10000
8000
6000
4000
2000
0
-2000
-15
-10
-5
0
5
10
15
angle (deg)
Vx = 1.6 m/s
Vx = 3.2 m/s
Vx = 4.8 m/s
Vx = 6.4 m/s
Vx = 8.0 m/s
Vx = 10. m/s